Plasma Science and Technology

PAPER

Measurement of radial temperature distributions of the blown CO_2 arcs under different conditions

Recent citations

- Evolution of anodic erosion components and heat transfer efficiency for W and $W_{80}Ag_{20}$ in atmospheric-pressure arcs
Yufei Cui *et al*

To cite this article: Yang LI *et al* 2019 *Plasma Sci. Technol.* **21** 125405

View the article online for updates and enhancements.

This content was downloaded from IP address 115.154.32.11 on 25/11/2020 at 13:40

© 2019 Hefei Institutes of Physical Science, Chinese Academy of Sciences and IOP Publishing Printed in China and the UK

Plasma Sci. Technol. **21** (2019) 125405 (7pp) https://doi.org/10.1088/2058-6272/ab40da

Measurement of radial temperature distributions of the blown CO_2 arcs under different conditions

Yang LI (李阳) , **Shaodi FAN** (范韶迪)[1], **Yi WU** (吴翊)[1], **Hao SUN** (孙昊), **Haodong CHANG** (畅浩栋), **Luqi LIANG** (梁璐奇) **and Weiping GUAN** (官玮平)

State Key Laboratory of Electrical Insulation and Power Equipment, Xi'an Jiaotong University, Xi'an 710049, People's Republic of China

E-mail: fanshaodi123@stu.xjtu.edu.cn and wuyic51@xjtu.edu.cn

Received 9 May 2019, revised 30 August 2019
Accepted for publication 3 September 2019
Published 1 October 2019

Abstract

In this paper, the radial temperature distributions of the blown CO_2 arcs in a model gas circuit breaker were investigated by optical emission spectroscopy methods. The CO_2 flows with different flow rates (50, 100 and 150 l min^{-1}) were created to axially blow the arcs burning in a polymethyl methacrylate (PMMA) nozzle. Discharges with different arc currents (200 and 400 A) were conducted in the experiment. The absolute intensity method was applied for a carbon ionic line of 657.8 nm to obtain the radial temperature profiles of the arc columns at a cross-section 1 mm above the nozzle. The calibration for the intensity of the C II 657.8 nm line was achieved by the Fowler–Milne method with the help of an oxygen atomic line of 777.2 nm. The highest temperature obtained in the arc center was up to 19 900 K when the arc current was 400 A and the CO_2 flow rate was 50 l min^{-1}, while the lowest temperature in the arc center was about 15 900 K when the arc current was 200 A and the CO_2 flow rate was 150 l min^{-1}. The results indicate that as the arc current increases, the temperature in the arc center would also increase apparently, and a larger gas flow rate would lead to a lower central temperature in general. It can also be found that the influence of the CO_2 flow rate on the arc temperature was much less than that of the arc current under the present experimental conditions. In addition, higher temperature in the arc center would cause a sharper temperature decrease from the central region towards the edge.

Keywords: blown CO_2 arc, optical emission spectroscopy, temperature distribution, absolute intensity method, Fowler–Milne method

(Some figures may appear in colour only in the online journal)

1. Introduction

Due to its outstanding performance, sulfur hexafluoride (SF_6) has been widely used as a gaseous dielectric and arc-quenching medium for high-voltage circuit breakers, switchgears and other electrical equipment in power transmission systems. However, SF_6 gas is also one of the most potent greenhouse gases whose global warming potential is 23 900 times higher than that of carbon dioxide (CO_2). As a consequence, it is important to reduce the usage of SF_6 gas. Great effort is being made to develop SF_6-alternative gases, and several CO_2-based candidates such as CO_2, CO_2–$C_5F_{10}O$, CO_2–CF_3I, C_3F_8–CO_2 and C_4F_7N–CO_2 [1–7] have already been proposed and studied in recent years.

Among these researches, optical diagnostics has attracted a lot of interests in the investigations of the composition and properties of arc plasmas, because of its non-intrusive feature, accuracy of measurement results and the maturity of related theories. Optical emission spectroscopy (OES) methods, such as the absolute intensity method, relative line intensity

[1] Authors to whom any correspondence should be addressed.

method, Boltzmann plot method and Fowler–Milne method, have also been widely developed and applied in the arc temperature measurements. By adopting the absolute intensity method for spectral lines F I 634.8, F I 641.3, C II 657.8 and C II 658.3 nm, Kozakov *et al* [8] obtained the radial arc temperature profiles in a polytetrafluoroethylene (PTFE) nozzle. Bai *et al* [9] measured three copper atomic spectral lines Cu I 510.5, Cu I 515.3 and Cu I 521.8 nm at different arc ignition time, to reveal the time-resolved axial arc temperature distributions by using the relative line intensity method. With the help of a CCD and filter devices, Takeuchi and Kubono [10] used the relative line intensity method for two copper atomic spectral lines (Cu I 465.1 and Cu I 515.3 nm), to calculate the temperature and the metal-vapor quantity in the cross-section of the arc column near the cathode. In order to study the temperature distribution of an argon arc, Ma *et al* [11] established a monochromatic imaging system with filter detectors. The temperature field of the argon arc was obtained by using the Fowler–Milne method for the argon atomic spectral line Ar I 798.4 nm. Xiao *et al* [12] used three different spectroscopic methods to calculate the temperature and composition distribution of argon-helium arc plasma, and analyzed the accuracy of different methods.

For high-voltage gas circuit breakers (GCBs), blowing gas plays an important role in the arc characteristics during the interruption process [13, 14]. The effects of blowing pressure or gas flow rate on the arc temperature are worthy of in-depth study. In our experiment, a model GCB with two graphite electrodes was adopted, the CO_2 gas flows with different flow rates (50, 100 and 150 l min^{-1}) were created to blow the arcs burning in a polymethyl methacrylate (PMMA) nozzle, and the discharges with different arc currents (200 and 400 A) were conducted. Based on the OES diagnostics, the radial temperature distributions of the blown CO_2 arc columns under different conditions are presented in this paper. The absolute intensity method was applied for a carbon ionic line of 657.8 nm (C II 657.8 nm) to obtain the radial temperature profiles of the arcs, while the line intensity calibration process was achieved by means of the Fowler–Milne method. The normal temperature of an oxygen atomic line of 777.2 nm (O I 777.2 nm) and its corresponding position were adopted for the calibration process.

2. Experimental setup

The experimental setup can be mainly divided into two parts according to different functions: Part 1: arc generating and extinguishing section; Part 2: spectral measuring and recording section. Figure 1 shows the schematic diagram of the experimental setup. A precise signal source (SRS DG535) with multi-outputs was used to generate transistor–transistor logic signals in sequence to trigger the equipment below, including the solid-state relay, the insulated gate bipolar transistor (IGBT), the high-speed camera and the ICCD.

2.1. Arc generating and extinguishing section

A continuously adjustable DC source was used as the power supply, and an IGBT was connected in parallel with the model GCB for commutating and interrupting the current. The model GCB was equipped with two vertically arranged graphite electrodes and placed in a stainless-steel cylindrical chamber with several ports for operation and observation. The upper electrode was the anode, which could be driven up and down through an insulated rod connected to a linear motor. The lower cathode was fixed and placed inside a PMMA nozzle. The contact parts of the anode and cathode were polished into a plane and cone, respectively. By using a mass flow controller, the CO_2 gas flows with different flow rates (50, 100 and 150 l min^{-1}) were created to axially blow the arcs. The details of the electrode setup and nozzle are shown in figure 2.

At the beginning of the experiment, the model GCB was closed and the CO_2 gas flow was created at a pre-set flow rate. The circuit current went through the IGBT branch first and then it was commutated to the GCB branch by turning off the IGBT. Once the anode was driven up by the linear motor, the arc would be generated between the two electrodes.

The arc began to burn in a steady state after the anode stopped at the proposed position. Then, about 10 ms later, the IGBT was turned on to commutate the arc current back to the IGBT branch, and the arc was extinguished accordingly.

2.2. Spectral measuring and recording section

As shown in figure 1, the spectrum section consisted of two convex lenses, two plane mirrors, a spectrometer (Andor SR500i) and an ICCD camera (iStar DH334T). Two lenses were used for imaging the arc column and two plane mirrors were placed between the lens group and the entrance slit of the spectrometer to serve as a beam steerer. When the electrodes were fully separated, the arc column was approximately cylindrically symmetric, so that it was ready to be captured by the spectroscopic system. As denoted in figure 3, the entrance slit width was set at 10 μm to select the cross-section 1 mm above the nozzle. The exposure time and gain level of the ICCD was set at 40 μs and 1000 for the measurement of the C II 657.8 nm, and 20 μs and 0 for the O I 777.2 nm, respectively.

Apart from the spectroscopic system, a high-speed camera (Phantom Micro M310) was placed near the view port of the chamber to record the burning arc. The parameters of the high-speed camera remained unchanged under different experimental conditions, so that the arc behavior can be compared with each other from the images.

The lower half of figure 3 shows two images processed by the spectrometer and the ICCD. They present the emission distribution in the spectral range from 648–666 nm and from 768–786 nm. They were measured at a cross-section of the arc column under an arc current of 400 A and a gas flow rate of 150 l min^{-1}. These images contain the data of wavelength, radial position (pixel number, 1024 pixels for 11 mm) and relative intensity (counts). The bright narrow regions

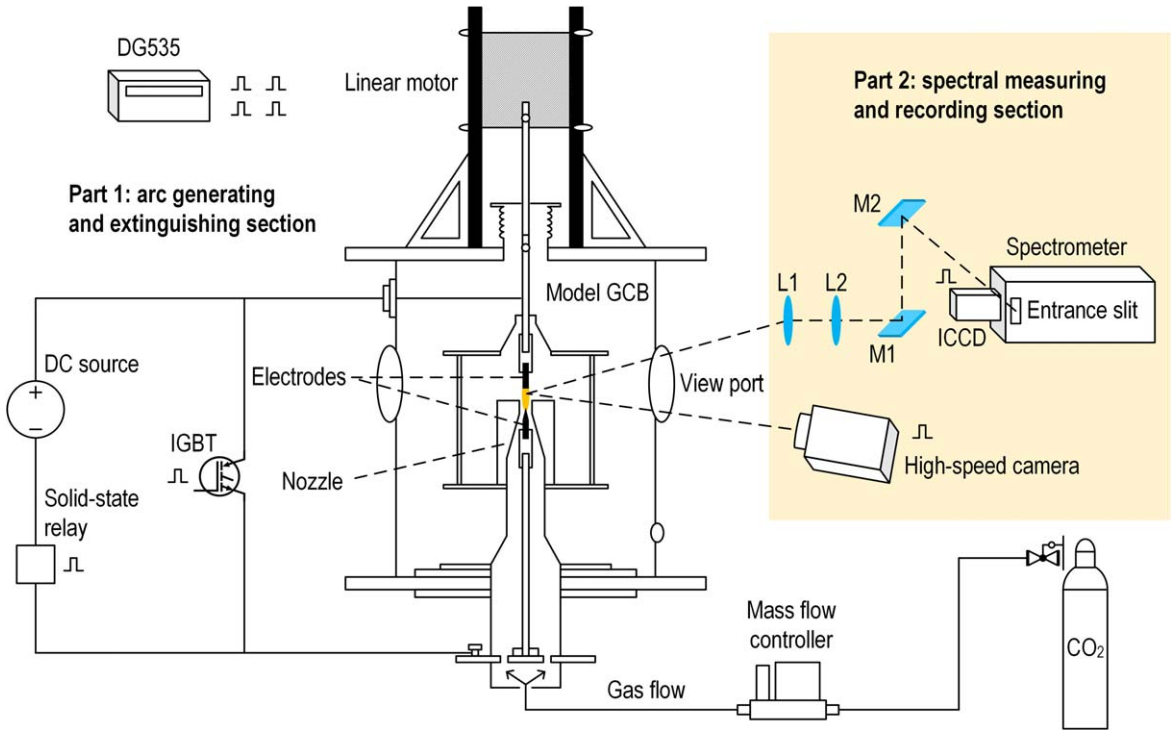

Figure 1. Schematic diagram of the experimental setup (M1, M2: plane mirrors, L1, L2: convex lenses).

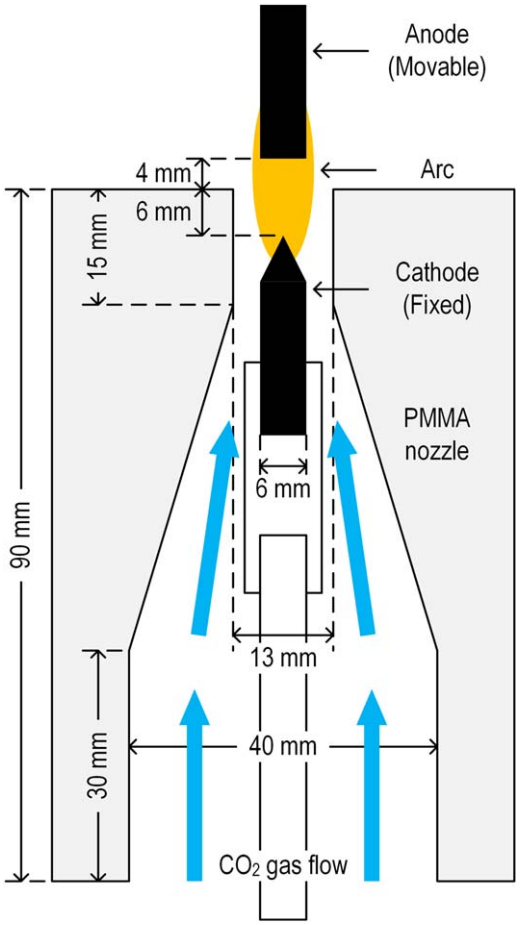

Figure 2. Electrode setup and profile of the nozzle.

correspond to the emission for spectral lines C II 657.8, C II 658.3, O I 665.38, O I 777.2 and O I 777.4 nm, respectively.

3. Temperature measurement methods

In this study, the C II 657.8 nm line was used by the absolute intensity method to calculate the temperature of the arc plasma, while the O I 777.2 nm line by the Fowler–Milne method to calibrate the emission intensity for the C II 657.8 nm line.

Based on the above, the radial dependence of the relative emission intensity and coefficient for the C II 657.8 nm line and O I 777.2 nm line is drawn in figure 4. It should be noted that the relative intensity (dots) in figure 4 is the optical measurement integrated along the line of sight, and it needs to be reconstructed. Assuming the arc column is cylindrically symmetric and optical thin, the relative emission intensity was converted to the relative emission coefficient (dash-dot line) by means of the Gaussian fitting method and Abel inversion [15, 16].

To understand the emission coefficient ε for a specific spectral line, equation (1) is given below:

$$\varepsilon = \frac{hc}{4\pi\lambda_{ul}} A_{ul} g_u \frac{N_j(T)}{Z_j(T)} \mathrm{e}^{-\frac{E_u}{kT}}, \tag{1}$$

where h, c and k are the Planck's constant, speed of light in vacuum and Boltzmann's constant, respectively; λ_{ul} and A_{ul} are the wavelength of the spectral line and the atomic transition probability; g_u and E_u are the statistical weight and the

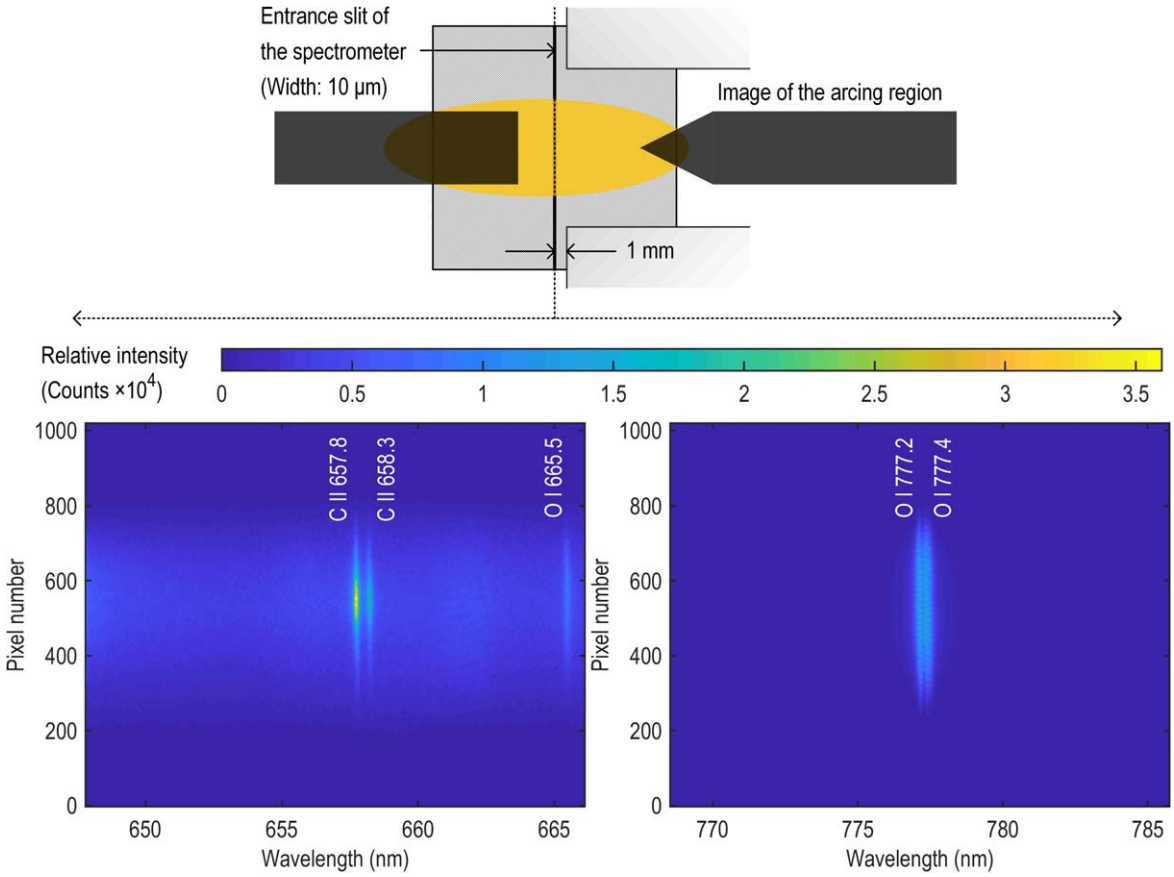

Figure 3. Specific cross-section of a steady arc column captured by the spectroscopic system.

energy of the upper level u of the species j [17]; N_j and Z_j are the number density and the partition function of the species j.

Assuming the arc plasma is in local thermodynamic equilibrium and at a constant pressure, N_j can be expressed as a function of the temperature T according to the mass action law, Dalton's law and the quasi-neutrality condition [18]. Z_j is also determined by the temperature T according to its definition expressed by the equation (2). For species j, E_i and g_i are the energy and the statistical weight of its energy level i.

$$Z_j = \sum_i g_i \mathrm{e}^{-\frac{E_i}{kT}}. \tag{2}$$

3.1. Fowler–Milne method

The Fowler–Milne method has been widely used in the OES diagnostics of arc plasma [11, 12, 19–21]. In this study, we applied this method to determine a calibration temperature and its corresponding position.

According to equations (1) and (2), the emission coefficients for spectral lines O I 777.2 and C II 657.8 nm under atmospheric pressure can be derived, as shown in figure 5. It can be seen that as the temperature varies from 0–40 000 K, the emission coefficient for different lines shows the same trend; it increases to a maximum value and then decreases. The maximum temperature of each emission coefficient curve is known as the normal temperature. In general, the temperature in the arc center is 15 000–20 000 K. As a result, the O I 777.2 nm line was chosen for the Fowler–Milne method in this study so that the off-axis maximum of the emission coefficient could be observed.

For the two off-axis maximum points in figure 4(b), the normal temperature of the O I 777.2 nm line is assigned. In theory, the absolute value of r_1 and r_2 should be equal, and the emission coefficient $\varepsilon_{\mathrm{rOI}}$ should be the same at both positions. However, the deviation from cylindrical symmetry, the measuring errors and the fitting errors cause a difference of 6.5% for the radial distance and 9.9% for $\varepsilon_{\mathrm{rOI}}$ in this example. In order to maintain the consistency, data from only the right side of each quasi-symmetric profile were adopted in the following calculations. Hence, the arc temperature at position r_2 is determined as 15 400 K under an arc current of 400 A and a gas flow rate of 150 l min^{-1}. This temperature and its corresponding position would be used for calibration.

3.2. Absolute intensity method

As mentioned above, the Fowler–Milne method is quite effective in the determination of the arc temperature. However, there are also limitations since the Fowler–Milne method relies on the obvious off-axis maximum of the emission intensity. That means the temperature in the arc center must be higher than the normal temperature, while it is

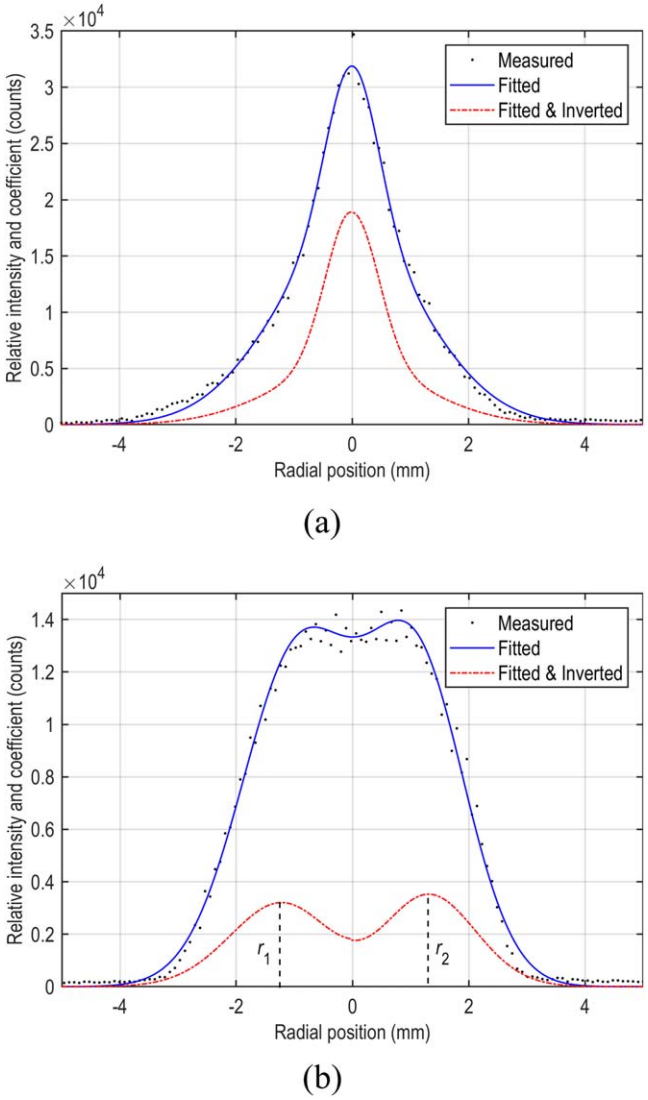

Figure 4. Radial dependence of relative emission intensity and coefficient for (a) C II 657.8 nm and (b) O I 777.2 nm (400 A, 150 l min^{-1}).

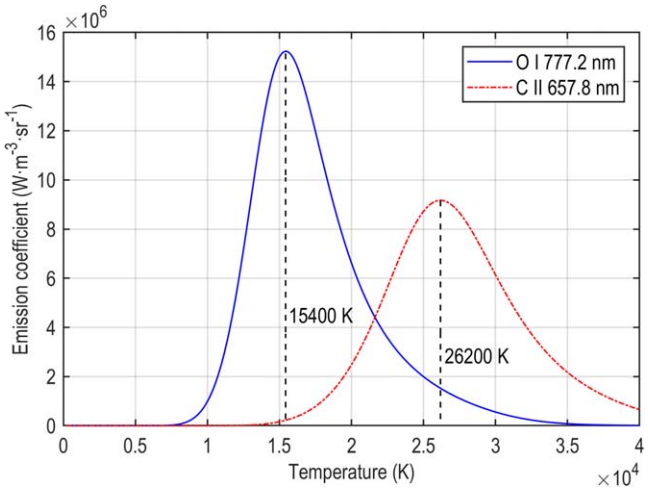

Figure 5. Calculated emission coefficient for spectral lines O I 777.2 and C II 657.8 nm.

not applicable for the low-current arcs. Hence, the absolute intensity method was adopted in our study to obtain the radial temperature distributions of the arcs under various experimental conditions.

The absolute intensity method derives the temperature from the absolute intensity for a spectral line. The emission intensity for the target spectral line should be strong enough to reduce the impact of measuring noises and errors, and it should also be separated from the intensity for other lines. In addition, the normal temperature should be high enough, so that the maximum emission intensity appears at the center of the radial profile and declines monotonously towards the edge. As a result, the emission intensity for the C II 657.8 nm line was chosen for the absolute intensity method.

Based on the absolute intensity method, the arc temperature can be determined by the left side of the emission coefficient ε (Unit: $W \cdot m^{-3} \cdot Sr^{-1}$) curve for C II 657.8 nm in figure 5. However, the emission coefficient ε_r (Unit: counts) in figure 4(a) is relevant to the spectroscopic system. In consequence, it is necessary to calculate the constant F defined as $\varepsilon = F \cdot \varepsilon_r$.

Considering the arc temperature of 15 400 K at position r_2 described in section 3.1, the emission coefficient ε for the C II 657.8 nm line at 15 400 K can be obtained from figure 5, and the relative emission coefficient ε_r at position r_2 can be obtained from figure 4(a). Thus, the constant F was calculated in a single case.

The calibration process was achieved by acquiring an averaged F in multiple measurements under an arc current of 400 A and a gas flow rate of 150 l min^{-1}. As the spectroscopic setup remained unchanged after the calibration, the arc temperature distribution under all experimental conditions can be derived by the absolute intensity method.

4. Results and discussion

Blown arcs under different experimental conditions are shown in figure 6; free-burning arcs are also presented as a comparison. It can be seen that the gas flow, even at a relatively small rate of 50 l min^{-1}, had a significant effect on the arc behavior, and the brightness of the arc column shows an obvious attenuation of temperature when the gas flow was introduced to the arc region. It also can be seen that the influence of the gas flow rate on the arc temperature was much less than that of the arc current.

Figure 7 shows temperature profiles of arc columns obtained under different arc currents and flow rates. The highest temperature appearing in the arc center was about 19 900 K when the arc current was 400 A and the CO_2 flow rate was 50 l min^{-1}, while the lowest temperature in the arc center was about 15 900 K when the arc current was 200 A and the CO_2 flow rate was 150 l min^{-1}. For a certain flow rate, the temperature difference in the arc center was up to 4000 K, while for a certain arc current, the temperature difference was no more than 1000 K. It should be noted that the temperature difference in the central region ($r < 1$ mm)

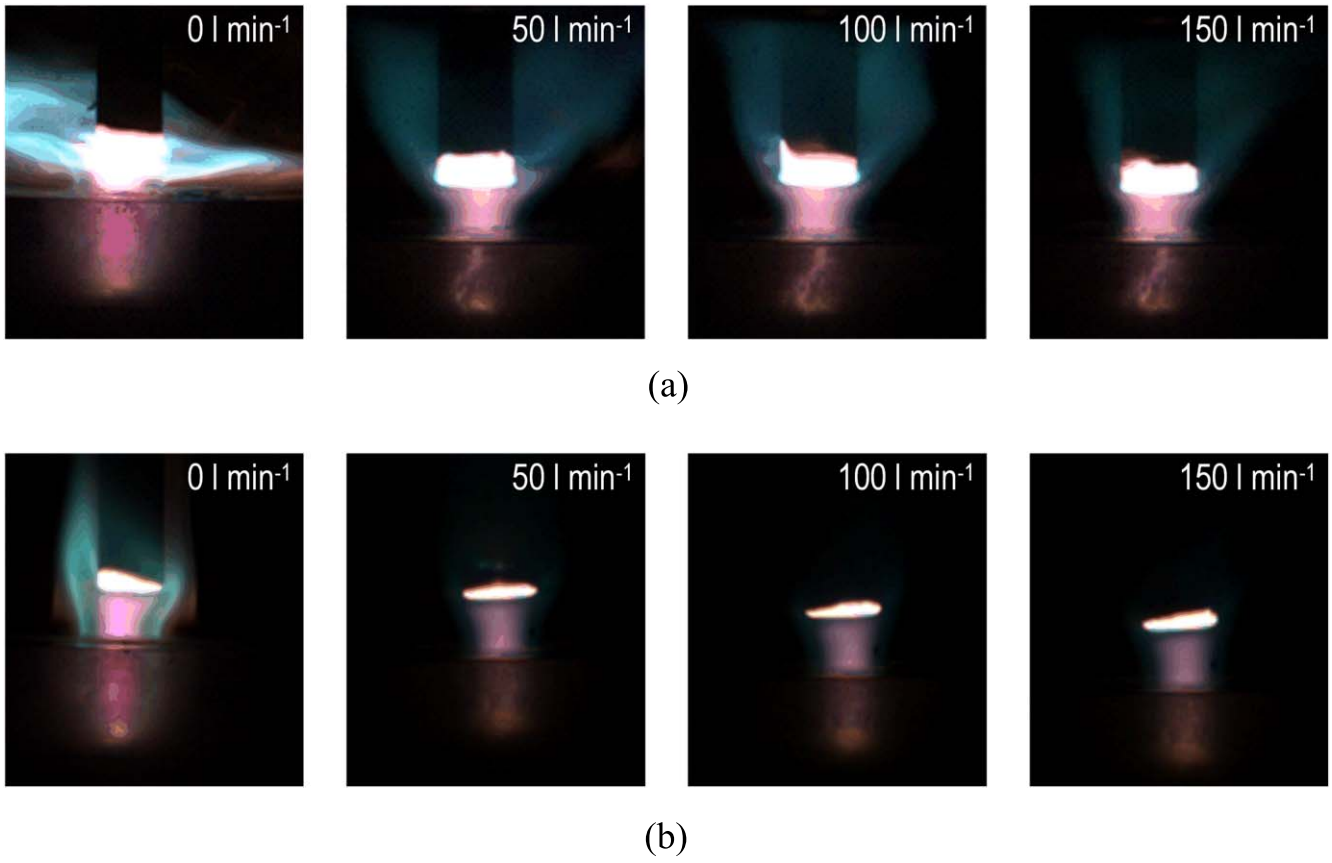

Figure 6. Burning arcs under different experimental conditions, (a) 400 A and (b) 200 A.

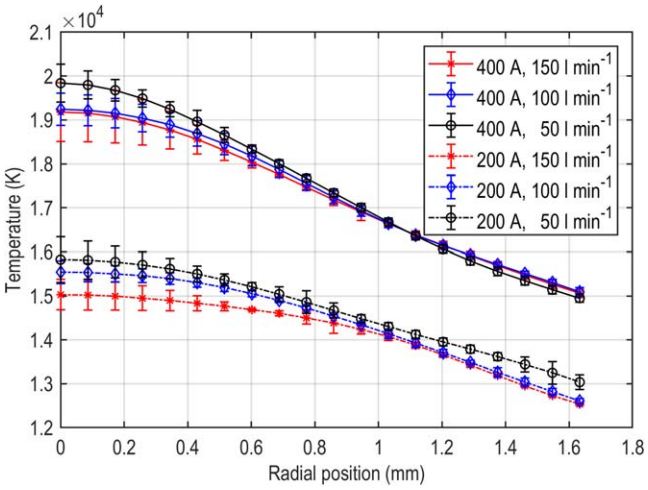

Figure 7. Temperature profiles of arc columns under different experimental conditions.

caused by different flow rates for 400 A was also smaller than that for 200 A. In other words, the influence of the gas flow rate on the arc temperature was much less than that of the arc current, and a higher arc current led to a smaller influence of the flow rates on the arc temperature.

The decrease of average temperatures from the arc center ($r = 0$) towards the edge ($r = 1$ mm) under different experimental conditions is listed in table 1.

Table 1. Decreases of average temperature under different experimental conditions.

	Temperature decrease		
Arc current	50 l min^{-1}	100 l min^{-1}	150 l min^{-1}
200 A	1525 K	1398 K	960 K
400 A	3164 K	2600 K	2540 K

From table 1 and figure 7, it is easy to draw the conclusion that higher temperature in the arc center would cause a sharper temperature decrease from the central region towards the edge. For example, the temperature decrease corresponding to 400 A was about 2–3 times that corresponding to 200 A for a certain flow rate. It should be noted that the temperature decrease for gas flow rates of 100 and 150 l min^{-1} was almost the same when the arc current was 400 A. That means for a high-current arc, the flow rate had a very small impact on the arc temperature distribution.

The phenomena mentioned above can be explained by the fact that too much Ohmic heating power was generated in the arc column with the increasing arc current, the arcing region in the nozzle was under high pressure and high temperature, blowing gas from the upstream region of the nozzle was blocked by the hot arc plasma so less cooling

power could be brought out. Consequently, the cooling mechanism of the blowing gas flow seemed to be weak.

The main sources of errors and uncertainties are listed as follows. First, the arc was considered to be steady when the OES acquisition was performed, although small fluctuations of the arc characteristics were inevitable. Second, in order to reconstruct the emission intensity, the axisymmetric assumption of the arc column was made. However, this assumption was usually not ideal and it led to the deviation of the final results. Finally, each temperature profile was an average of three repetitive experiments, and errors caused by the repeatability of the experiment cannot be avoided completely.

5. Conclusions

In this paper, the radial temperature distributions of the DC blown CO_2 arcs in a model GCB were investigated by OES methods. The Fowler–Milne method for the O I 777.2 nm line was adopted to calibrate the emission intensity for the C II 657.81 nm line, which was adopted by the absolute intensity method. Quantitative results of the temperature distribution under different conditions were obtained by the absolute intensity method.

It is found that the influence of the gas flow rate on the arc temperature is much less than that of the arc current. A higher arc current would lead to a smaller influence of the flow rates on the arc temperature. In addition, with a higher central temperature in the arc center, a sharper temperature decrease from the central region towards the edge would appear.

Acknowledgments

This work was supported by National Natural Science Foundation of China (Nos. 51577145, 51707144 and 51877165), the Key Research and Development Program of Shaanxi Province (No. 2018ZDXM-GY-112) and the State Key Laboratory of Electrical Insulation and Power Equipment (No. EIPE19302).

ORCID iDs

Yang LI (李阳) https://orcid.org/0000-0001-5878-1258

References

[1] Sun H *et al* 2015 *J. Phys. D: Appl. Phys.* **48** 055201
[2] Guo Z *et al* 2019 *IEEE Trans. Plasma Sci.* **47** 2742
[3] Widger P, Griffiths H and Haddad A 2018 *IEEE Trans. Dielectr. Electr. Insul.* **25** 330
[4] Zhao X L, Yan J D and Xiao D M 2018 *Plasma Sci. Technol.* **20** 085404
[5] Stoller P C *et al* 2017 *IEEE Trans. Dielectr. Electr. Insul.* **24** 2712
[6] Deng Y K, Li B and Xiao D M 2015 *IEEE Trans. Dielectr. Electr. Insul.* **22** 3253
[7] Okubo H and Beroual A 2011 *IEEE Electr. Insul. Mag.* **27** 34
[8] Kozakov R *et al* 2007 *J. Phys. D: Appl. Phys.* **40** 2499
[9] Bai S *et al* 2018 *IEEE Trans. Plasma Sci.* **46** 2120
[10] Takeuchi M and Kubono T 2000 *IEEE Trans. Plasma Sci.* **28** 991
[11] Ma S L *et al* 2011 *J. Phys. D: Appl. Phys.* **44** 405202
[12] Xiao X, Hua X M and Wu Y X 2015 *Opt. Laser Technol.* **66** 138
[13] Thomas J, Chaffey G P and Franck C M 2017 *IEEE Trans. Compon. Pack. Manuf. Technol.* **7** 1058
[14] Panousis E, Bujotzek M and Christen T 2014 *IEEE Trans. Power Deliv.* **29** 1806
[15] Vilarinho L O and Scotti A 2004 *J. Braz. Soc. Mech. Sci. Eng.* **26** 34
[16] Bockasten K 1961 *J. Opt. Soc. Am.* **51** 943
[17] Kramida A 2018 *NIST atomic spectra database: NIST standard reference database 78* (https://doi.org/10.18434/T4W30F) (Accessed: 5 August 2019)
[18] Wu Y *et al* 2016 *J. Phys. D: Appl. Phys.* **49** 405203
[19] Murphy A B 1994 *Rev. Sci. Instrum.* **65** 3423
[20] Bachmann B *et al* 2013 *J. Phys. D: Appl. Phys.* **46** 125203
[21] Pokrzywka B *et al* 1996 *J. Phys. D: Appl. Phys.* **29** 2644